Available online at www.sciencedirect.com

SCIENCE DIRECT®

Journal of Molecular Catalysis A: Chemical 204–205 (2003) 629–635

JOURNAL OF MOLECULAR CATALYSIS A: CHEMICAL

www.elsevier.com/locate/molcata

Preparation, characterisation and activity of CeO_2-ZrO_2 catalysts for alcohol dehydration

V. Solinas [a,*], E. Rombi [a], I. Ferino [a], M.G. Cutrufello [a], G. Colón [b], J.A. Navío [b]

[a] *Dipartimento di Scienze Chimiche, Università di Cagliari, Complesso Universitario Monserrato, s.s. 554 Bivio Sestu, 09042 Monserrato (Ca), Italy*

[b] *Instituto de Ciencia de Materiales, Centro de Investigaciones Cientificas (Isla de la Cartuja), Centro Mixto CSIC-Universidad de Sevilla, Avda. Américo Vespucio s/n, 41092 Sevilla, Spain*

Received 24 September 2002; received in revised form 29 January 2003; accepted 14 February 2003

Dedicated to Professor Renato Ugo on the occasion of his 65th birthday

Abstract

Ceria-zirconia catalysts with 100, 75, 50, 25 and 0 mol% of ceria have been prepared and characterised by X-ray diffraction, Raman spectroscopy, N_2 physisorption, transmission electron microscopy, X-ray photoelectron spectroscopy and adsorption microcalorimetry of probe molecules. All the catalysts have been tested for the conversion of 4-methylpentan-2-ol into 4-methylpent-1-ene, valuable monomer for plastics manufacture. Steady-state 1-alkene selectivity values ranging between 84 and 59% have been observed. The catalytic behaviour has been interpreted on the basis of competing E1cB, E1 and E2 mechanisms, a well balanced concentration of the acid and basic sites with a high strength of the latter being required for optimum performance.

Keywords: Ceria; Zirconia; Acid–base; Alcohol; Dehydration

1. Introduction

Ceria has been thoroughly investigated [1] mainly because of its use as an active component of three-way catalysts for the treatment of exhaust gases. In recent years, special attention has been focused on the preparation of ceria-zirconia solid solutions [2–4]. Despite their key role in several catalytic applications, little has been published about the acid–base properties of ceria [5–8] and ceria-zirconia solid solutions [9]. Among the acid–base catalysed reactions on metal oxides, the conversion of 4-methylpentan-2-ol into 4-methylpent-1-ene deserves particular attention, the latter being the monomer for the manufacture of thermoplastic polymers of superior technological properties.

In the present paper, ceria-zirconia mixed oxides have been prepared in a wide composition range via a sol–gel co-precipitation route. The catalysts have been characterised as to their structural, textural and surface properties, including the acid and base features, by a variety of techniques. The catalytic behaviour in the conversion of 4-methylpentan-2-ol has been investigated on the grounds of the physico-chemical characterisation data.

* Corresponding author. Tel.: + 39-070-675-4384: fax: +39-070-675-4388.
E-mail address: solinas@unica.it (V. Solinas).

1381-1169/$ – see front matter © 2003 Elsevier Science B.V. All rights reserved.
doi:10.1016/S1381-1169(03)00347-9

2. Experimental

Pure ceria (Ce100), pure zirconia (Zr100) and cerium-zirconium mixed oxides (Ce75Zr25, Ce50-Zr50, Ce25Zr75) were prepared via sol–gel (the figures after each symbol refer to the mol% content of the corresponding oxide). Nitrate precursors, $Ce(NO_3)_3{\cdot}6H_2O$ and $ZrO(NO_3)_2{\cdot}xH_2O$, were supplied by Aldrich. Appropriate amounts of each nitrate were mixed in distilled water and aqueous ammonia was added until pH reached a value of 9. The gel thus obtained was filtered and dried at 110 °C overnight. The final catalyst was obtained by calcining the powder at 600 °C for 2 h.

All the catalysts were characterised by X-ray diffraction, Raman spectroscopy, nitrogen physisorption, transmission electron microscopy (TEM), X-ray photoelectron spectroscopy (XPS). XRD patterns were recorded on a Siemens D-591 diffractometer (Cu Kα radiation, Ni filter, graphite monochromator). Raman spectra were recorded on a Nicolet 910 instrument equipped with a Nd:YAG laser (1064 nm), a Ge detector and 180° refractive configuration. Both XRD and Raman analysis were carried out also on samples calcined for 2 h at 800 and 1000 °C. Nitrogen adsorption–desorption experiments were carried out at −196 °C on a Micromeritics 2000 instrument and a Philips CM200 microscope was used for TEM investigation. The XPS study was carried out on a Leybold–Haereus LHS-10 spectrometer, working with a constant pass energy of 50 eV; Mg Kα radiation was used for excitation ($h\nu$ = 1253.6 eV). Further details can be found elsewhere [10].

The acid and base properties have been assessed by adsorption microcalorimetry of probe basic and acidic molecules (NH_3 and CO_2, respectively) by means of a Tian–Calvet heat flow equipment (Setaram). Each sample was evacuated (10^{-3} Pa) overnight at 400 °C and then kept at 80 °C during the stepwise introduction of small doses of the probe gas (ammonia or carbon dioxide). Details on the apparatus and procedure can be found in [11]. Catalytic testing was carried out at atmospheric pressure in a quartz-made fixed-bed flow microreactor after in situ activation for 6 h at 500 °C under CO_2-free air flow. Reaction conditions were: carrier gas, N_2; partial pressure of alcohol, 1.9×10^4 Pa; time factor, 0.54 $g_{catalyst}$ h/$g_{alcohol}$. Detailed procedure and analytical conditions are reported in [11].

3. Results and discussion

3.1. Structure, texture and surface composition

The XRD patterns of the catalysts are shown in Fig. 1. They can be assigned to the fluorite cubic structure in the case of pure ceria and to a mixture of monoclinic and tetragonal phases in the case of pure zirconia (monoclinic mole fraction = 0.7). The identification of such phases is confirmed by the Raman spectra in Fig. 2 [12,13]. The phase assignment for the mixed oxides is less straightforward. Cubic, tetragonal and monoclinic structures have been reported for ceria-zirconia solid solutions [12,14,15]. The XRD patterns for Ce25Zr75, Ce50Zr50 and Ce75Zr25 (Fig. 1) seem to indicate cubic phases similar to ceria, the shift of the peaks towards higher 2θ values being due to the small ionic radius of Zr^{4+} in comparison with that of Ce^{4+}. Only one phase can be identified in Ce25Zr75, but the high-2θ shoulders in the XRD patterns of Ce50Zr50 and Ce75Zr25 reveal

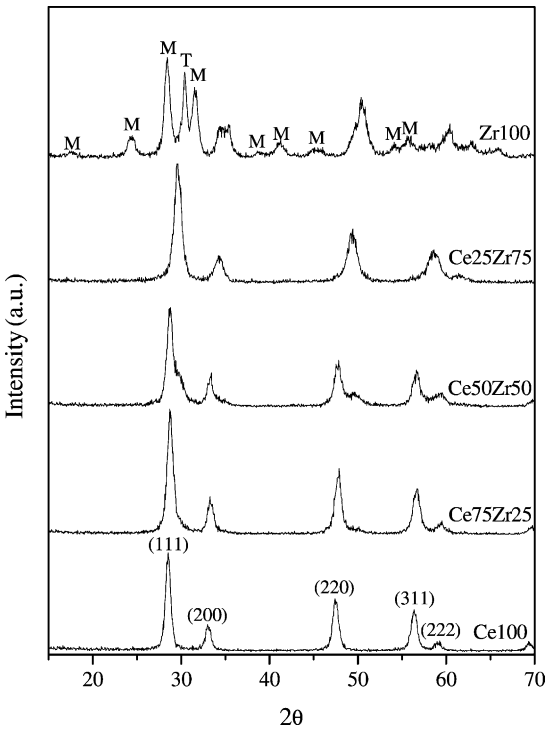

Fig. 1. XRD patterns for ceria-zirconia catalysts. M, monoclinic; *T*, tetragonal.

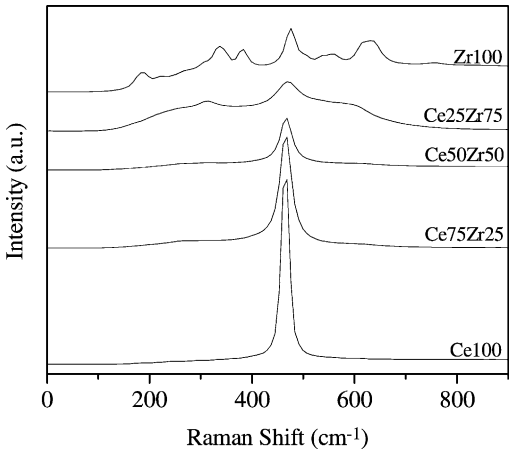

Fig. 2. Raman spectra for ceria-zirconia catalysts.

the presence of a minor zirconia-rich phase (also confirmed by XRD data of the samples calcined at 800 and 1000 °C, not reported for brevity). The Raman spectra of these two catalysts (Fig. 2) show a band at 465 cm^{-1}, typical of a cubic structure [4]. On the contrary, Ce25Zr75 spectrum indicates that such a catalyst has a tetragonal structure which, unlike XRD, Raman spectroscopy can easily distinguish from the cubic one [15]. Traces of the bands typical of the Ce25Zr75 phase, which seem to be present in the Raman spectra of Ce50Zr50 and Ce75Zr25, have been clearly seen after calcination at 1000 °C, not reported for brevity. This suggests that, though the fluorite-type structured cubic solid solution is by far predominant, the zirconia-rich solid solution present in Ce50Zr50 and (in traces) in Ce75Zr25 has a tetragonal structure similar to Ce25Zr75. The textural features of the samples are summarised in Table 1.

Table 2
Binding energies (eV) for the Ce 3d and O 1s levels and surface chemical composition (Ce mol%) of ceria-zirconia catalysts

Catalyst	Binding energy Ce 3d	Binding energy O 1s	Ce content
Ce100	917.0	529.5	100
Ce75Zr25	917.0	529.4	91
Ce50Zr50	917.0	529.5	79
Ce25Zr75	917.0	529.9	41
Zr100		530.2	

X-ray photoelectron spectra of Ce 3d, Zr 2p and O 1s were recorded for all the catalysts. A summary of the results is presented in Table 2. The cerium binding energy is typical of fully oxidised material [10]. The binding energy for O 1s is slightly higher for Ce25Zr75 than for the other mixed oxides, i.e. a change in the polarisation of the metal–oxygen bond occurs for the sample with the lowest ceria content. By peak integration (taking into account the sensitivity factor for each element) the surface chemical composition of the mixed oxides was assessed. The values reported in Table 2 clearly indicate that cerium enrichment occurs at the surface. Such a phenomenon has already been reported for a similar system prepared by sol–gel; it is probably originated by the differences in the charge-to-radius ratio between Ce^{3+} and Zr^{4+}, which would result in a sequential precipitation process from sol to gel [3].

3.2. Acidity and basicity

Calorimetric results are summarised in Fig. 3, where the differential heat of adsorption (Q_{diff}) is plotted versus ammonia and carbon dioxide uptake.

Table 1
Textural and morphological properties of ceria-zirconia catalysts

Catalyst	Isotherm type[a]	Surface area[b] (m^2/g)	Pore volume (cm^2/g)	Pore diameter[c] (nm)	Particle size[d] (nm)
Ce100	IV	35.6	0.0765	3.5; 8.0	15.4
Ce75Zr25	IV	52.7	0.1025	3.5; 7.5	10.6
Ce50Zr50	IV	40.4	0.0619	3.5; 6.0	10.1 (6.5)
Ce25Zr75	IV	12.3	0.0136	3.5	5.5
Zr100	IV	40.0	0.0848	3.5; 5.0	11.9

[a] Brunauer classification [16].
[b] BET method.
[c] Most frequent diameters (BJH method).
[d] Calculated by the Scherrer formula from the XRD profiles; the value within brackets refers to the minor phase. TEM images show roundish particles, whose dimensions are in agreement with those obtained from XRD analysis.

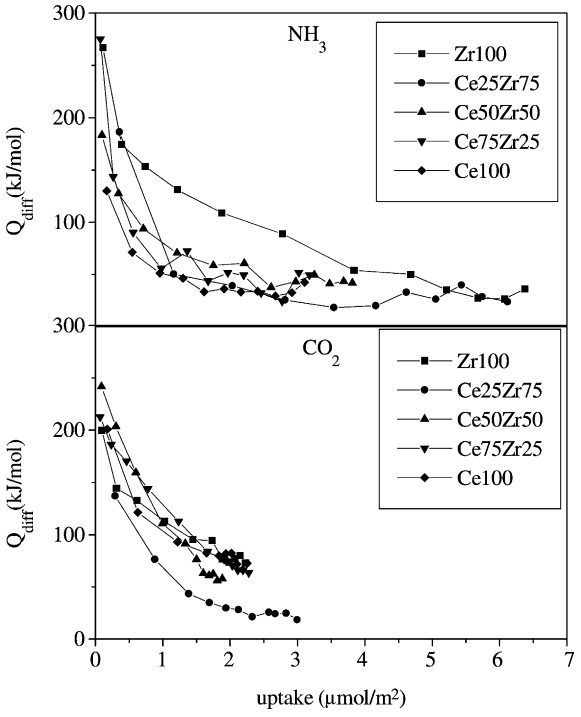

Fig. 3. Differential heat of adsorption, Q_{diff} vs. ammonia and carbon dioxide uptake for ceria-zirconia catalysts.

For all the samples Q_{diff} decreases as the adsorbed amount of ammonia increases, with a smoother trend in the case of zirconia. The adsorption profiles for the mixed oxides lie above that for ceria and below that for zirconia, being somewhat closer to the former than to the latter. The curves for CO_2 adsorption also show a continuously decreasing trend. The profiles for ceria and zirconia do not differ so markedly as in the case of NH_3 adsorption. Interestingly, the curve of Ce25Zr75 lies below those of all the other samples. Chemical adsorption of ammonia and carbon dioxide occurs at the acidic and basic sites, respectively. The former are coordinatively unsaturated (c.u.s.) metal cations and the latter c.u.s. oxygen anions. The Q_{diff} versus CO_2 uptake profile for ceria (Fig. 3) reveals that no families of sites of the same energy are present on the surface. This energetic heterogeneity of the oxygen anions should stem from structural reasons, i.e. differences in the particular crystallographic configuration of the oxygen ions (at step, kink and edge positions). The energetic heterogeneity of the CO_2-adsorbing sites observed for the mixed oxides (Fig. 3) could be due not only to structural reasons but also to chemical differences among the oxygen anions, Ce- and Zr-bonded oxygens being simultaneously present. Such a chemical heterogeneity would be revealed by changes in the binding energy values of O 1s in the XPS spectra. In this respect, two points are worthy noting. (i) For Ce100, Ce75Zr25, Ce50Zr50 (where the fluorite-type structure typical of ceria is maintained as the zirconium content in the lattice increases) the binding energy corresponding to the O 1s peak is practically the same (Table 2), and the Q_{diff} versus CO_2 uptake profiles show only minor differences (Fig. 3). (ii) When the cubic structure is abandoned and the solid solution assumes a tetragonal structure (Ce25Zr75), the O 1s signal shifts to a binding energy higher than that for the above-cited samples, but lower than that for Zr100 (Table 2); in parallel, the Q_{diff} versus CO_2 uptake appears significantly different from those of Ce100, Ce75Zr25, Ce50Zr50, on one hand, and from that of Zr100, on the other (Fig. 3). It seems that chemical heterogeneity among the c.u.s. oxygen ions can manifestly develop only when the situation outlined in (ii) is attained.

3.3. Catalytic behaviour

The transformation of 4-methylpentan-2-ol over the present samples gave dehydration and dehydrogenation products, the former being by far predominant. 4-Methylpent-1-ene (1-A, desired product) was the most abundant among the dehydration products; 4-methylpent-2-ene (2-A) and trace amounts of skeletal isomers of C_6 alkenes (C_6) were also formed. Dehydrogenation led to 4-methylpentan-2-one (K); high molecular weight ketones (HK) were formed only in trace amounts.

The reactant alcohol conversion and the selectivity to the various products, S_i (i = 1-A, 2-A, C_6, K, HK), were monitored as a function of time-on-stream for each catalyst. Runs carried out at several reaction temperature levels showed, for all the catalysts, that while conversion increases with increasing temperature, selectivities do not depend on it. To evaluate the catalyst performance, the S_i values during an isothermal long-lasting (80 h) run, carried out at a temperature giving 50% conversion (T_{50}), have been considered. The case of Ce50Zr50 is shown in Fig. 4 as an example. From such plots average values of S_i

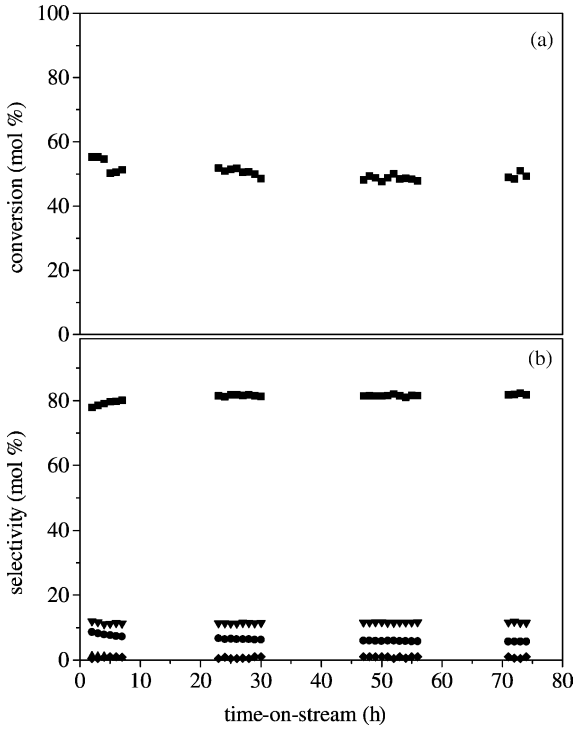

Fig. 4. (a) Conversion and (b) selectivities vs. time-on-stream for Ce50Zr50 catalyst at 360 °C. Symbols in (a and b): squares, 4-methylpent-1-ene; circles, 4-methylpent-2-ene; diamonds, skeletal isomers of C_6 alkenes with internal double bond; reversed triangles, 4-methylpentan-2-one; triangles, high molecular-weight ketones.

(calculated after attaining of stable behaviour) have been obtained for each catalyst; these are listed in Table 3, where T_{50} values are also reported. The best results in terms of 1-alkene selectivity are observed on Ce75Zr25 ($S_{1\text{-A}} = 84\%$) and Ce50Zr50 ($S_{1\text{-A}} = 82\%$); zirconia is a poor catalyst ($S_{1\text{-A}} = 59\%$).

Table 3
Catalytic activity of ceria-zirconia catalysts

Catalyst	T_{50} (°C)[a]	Selectivity (mol%)[b]				
		1-A	2-A	C_6	K	HK
Ce100	390	79	8	0	12	1
Ce75Zr25	365	84	5	0	9	2
Ce50Zr50	360	82	6	0	11	1
Ce25Zr75	375	74	9	1	16	0
Zr100	320	59	34	2	5	0

The data refer to later time-on-stream (>20 h) values.

[a] Temperature for 50% conversion.

[b] 1-A, 4-methylpent-1-ene; 2-A, 4-methylpent-2-ene; C_6, skeletal isomers of C_6 alkenes with internal double bond; K, 4-methylpentan-2-one; HK, high molecular-weight ketones.

3.4. Reaction pathways

The first step of alcohol transformation on metal oxides is the adsorption of the reactant alcohol on the surface. The adsorbed alcohol species can be converted through a two-step mechanism involving intermediate carbocation formation (E1), a concerted pathway (E2) or via carbanion formation mechanism (E1cB) [17]. (These mechanisms should be regarded as limiting cases, since intermediate situations can occur). According to previous findings from the present authors laboratories on several metal oxide catalysts [11,18], it can be proposed that the competition among E1, E2 and Ec1B mechanisms depends on the combined influence of: (i) the n_B:n_A ratio (where n_B and n_A represent the concentration of the basic and acid sites, respectively); (ii) the values of $n_{A\geq 80}$:n_A (fraction of sites with differential heat for ammonia adsorption $\geq$80 kJ/mol) and $n_{B\geq 80}$:n_B (fraction of sites with differential heat for carbon dioxide adsorption $\geq$80 kJ/mol). The former indicates whether the acid and basic functions are balanced or not, the latter informs about the relative strengths of the basic and acid sites; both suggest the adsorption mode of the alcohol and the timing of the bond ruptures, as outlined in the following.

The values of n_B:n_A, $n_{B\geq 80}$:n_B and $n_{A\geq 80}$:n_A, calculated for all the catalysts from Fig. 3 data (by neglecting the contribution of the physical adsorption as described in [11]) are reported in Table 4. In this same table the initial (1 h on-stream) S_i values, which represent the catalyst behaviour before the possible occurrence of surface modifications originating during the run, are also reported. For Ce100, Ce75Zr25 and Ce50Zr50, the acid and base functions are well balanced as to the number of sites (n_B:$n_A = 1$, 1 and 0.9, respectively), which would allow the reactant alcohol to be adsorbed via a two-point mechanism, involving the interaction of a surface basic site with an H atom of the methyl group and of a surface acid site with the O atom of the hydroxy group. The higher strength of the basic sites in comparison with that of the acid centres ($n_{B\geq 80}$:n_B and $n_{A\geq 80}$:n_A are 81 and 23%, respectively, for Ce100; 76 and 31% for Ce75Zr25; 78 and 46% for Ce50Zr50) would favour

Table 4
Acid–base properties and initial (1 h on-stream) reaction selectivities for ceria-zirconia catalysts

Catalyst	n_A (μmol/m^2)	n_B (μmol/m^2)	n_B:n_A	$n_{B\geq 80}$:n_B (%)	$n_{A\geq 80}$:n_A (%)	Selectivity[a] (mol%)		
						1-A	2-A + C_6	K + HK
Ce100	2.11	2.10	1.0	81	23	74	13	13
Ce75Zr25	2.21	2.27	1.0	76	31	81	8	11
Ce50Zr50	2.10	1.89	0.9	78	46	77	11	12
Ce25Zr75	2.01	1.39	0.7	61	49	62	20	18
Zr100	5.21	2.23	0.4	80	59	50	48	2

[a] 1-A, 4-methylpent-1-ene; 2-A + C_6, 4-methylpent-2-ene + skeletal isomers of C_6 alkenes with internal double bond; K + HK, 4-methylpentan-2-one + high molecular-weight ketones.

the C–H bond rupture leading to carbanion formation, from which OH is released to give the 1-alkene (Hofmann product, E1cB mechanism). As expected on these grounds, a very high selectivity towards the desired 1-alkene is observed for Ce100, Ce75Zr25 and Ce50Zr50 ($S_{1\text{-A}} = 74$, 81 and 77%, respectively). As usually happens when the E1cB mechanism is operating [17], also dehydrogenation takes place to some extent (S_{K+HK} (%) = 13, 11 and 12), as a consequence of hydride ion elimination (instead of OH^-) from the carbanionic species. For zirconia, the acid and basic site concentrations are imbalanced (n_B:$n_A = 0.4$), which makes possible the occurrence of E1 mechanism: attack of an acid site on the OH group of the reactant alcohol, carbocation formation, proton release from the latter to give the corresponding alkene with internal double bond (Saytzeff product). Expectedly, a remarkable selectivity to the undesired alkenes is observed ($S_{2\text{-A}+C6} = 48\%$), while 4-methylpentan-2-one selectivity becomes negligible ($S_{K+HK} = 2\%$). The presence of skeletal isomers of C_6 olefins ($S_{C6} = 6\%$), indicates the occurrence (to very low extent) of carbocation isomerisation on the acid sites of this catalyst, a remarkable fraction of which (59%) is stronger than 80 kJ/mol. The adsorption mode and the timing of the bond ruptures cannot be individuated in a such clear-cut way for Ce25Zr75. Both the acid–base features and the selectivity data for this catalyst are somewhat mid-way between those for ceria and the other mixed oxides, on one hand, and those for pure zirconia, on the other. The n_B:n_A ratio (0.7) is too high for a pure E1 mechanism, but not enough for allowing pure E1cB to set in; both mechanisms probably operate simultaneously. (It should be added that the 2-alkene might also form via an E2-like mechanism involving an activated complex with carbanionic character, instead of coming from the E1cB pathway; such a possibility is suggested by the $n_{B\geq 80}$:n_B and $n_{A\geq 80}$:n_A values (61 and 49%, respectively), which indicate that, though the basic sites are significantly stronger than the acid ones, the difference in strength is not as remarkable as for the other mixed oxides).

It has been already pointed out that the peculiar structural features of Ce25Zr75 (revealed by XRD and Raman) are accompanied by some specificity in its surface properties (from XPS and calorimetry). Though the influence of these properties on the catalytic behaviour cannot be described in detail, the selectivity data for Ce25Zr75, stemming from its peculiar acid–base features, confirm that this sample is different from ceria and the other mixed oxides, on one hand, and pure zirconia, on the other.

References

[1] A. Trovarelli (Ed.), Catalysis by Ceria and Related Materials, Imperial College Press, London, 2002.
[2] J. Kaspar, P. Fornasiero, M. Graziani, Catal. Today 50 (1999) 285.
[3] A. Martinez-Arias, M. Fernández-García, V. Ballestros, L.N. Salamanca, J.C. Conesa, C. Otero, J. Soria, Langmuir 15 (1999) 4796.
[4] G. Colón, M. Pijolat, F. Valdifieso, H. Vidal, J. Kaspar, E. Finocchio, M. Daturi, C. Binet, J.C. Lavalley, R.T. Baker, S. Bernal, J. Chem. Soc., Faraday Trans. 94 (1998) 3717.
[5] V.R. Choudary, V.H. Rane, J. Catal. 130 (1991) 411.
[6] K. Thomke, in: G.C. Bond, P.B. Wells, F.C. Thomkins (Eds.), Proceedings of the Sixth International Congress on Catalysis, The Chemical Society, London, vol. 1, 1977, p. 105.

[7] A. Auroux, P. Artizzu, I. Ferino, R. Monaci, E. Rombi, V. Solinas, G. Petrini, J. Chem. Soc., Faraday Trans. 92 (1996) 2619.
[8] P. Käßner, M. Baerns, Appl. Catal. 139 (1996) 107.
[9] M.G. Cutrufello, I. Ferino, V. Solinas, A. Primavera, A. Trovarelli, A. Auroux, C. Picciau, Phys. Chem. Chem. Phys. 1 (1999) 3369.
[10] G. Colón, J.A. Navío, R. Monaci, I. Ferino, Phys. Chem. Chem. Phys. 2 (2000) 4453, and literature cited therein.
[11] M.G. Cutrufello, I. Ferino, R. Monaci, E. Rombi, V. Solinas, Top. Catal. 19 (2002) 225, and literature cited therein.
[12] P. Fornasiero, G. Balducci, R. Di Monte, J. Kašpar, V. Sergo, G. Gubitosa, A. Ferrero, M. Graziani, J. Catal. 164 (1996) 173.
[13] D.A. Ward, E.I. Ko, Chem. Mater. 5 (1993) 956.
[14] E. Tani, M. Yoshimura, Sõmiya, J. Am. Ceram. Soc. 66 (1983) 506.
[15] M. Yashima, H. Arashi, M. Kakihana, M. Yoshimura, J. Am. Ceram. Soc. 77 (1994) 1067.
[16] F. Rouquerol, J. Rouquerol, K. Sing, Adsorption by Powders and Porous Solids, Academic Press, London, 1998, p. 18.
[17] J.M. Winterbottom, Catalysis, Specialist Periodical Reports, vol. 4, The Royal Society of Chemistry, London, 1981, Chapter 6, p. 141.
[18] M.G. Cutrufello, I. Ferino, R. Monaci, E. Rombi, V. Solinas, Stud. Surf. Sci. Catal. 140 (2001) 175.